NANO · MICRO small
www.small-journal.com

A Biogenic Photovoltaic Material

Sarvesh Kumar Srivastava, Przemyslaw Piwek, Sonal R. Ayakar, Arman Bonakdarpour, David P. Wilkinson, and Vikramaditya G. Yadav**

A proof-of-concept for the fabrication of genetically customizable biogenic materials for photovoltaic applications is presented. *E. coli* is first genetically engineered to heterologously express the carotenoid biosynthetic pathway from plants. This modification yields a strain that overproduces the photoactive pigment lycopene. The pigment-producing cells are then coated with TiO_2 nanoparticles via a tryptophan-mediated supramolecular interface, and subsequent incorporation of the resulting biogenic material (cells@TiO_2) as an anode in an I^-/I_3^--based dye-sensitized solar cell yields an excellent photovoltaic (PV) response. This work lays strong foundations for the development of bio-PV materials and next-generation organic optoelectronics that are green, inexpensive, and easy to manufacture.

1. Introduction

The transition from inorganic to organic photosensitive materials has been a significant milestone in the evolution of photovoltaic materials and dye-sensitized solar cells (DSSCs).[1–3] While the former exploit properties of solid-state semiconductors such as Si, GaAs, and CIS to generate photoinduced electron–hole pairs, the latter synergize the properties of semiconductors such as TiO_2 nanoparticles (NPs) and photoexcitable dyes.[4–6] More generally, organic DSSCs[7] are fabricated by immobilizing ruthenium-based light-absorbing chelates over a titania (TiO_2)-based working electrode in the presence of an electrolyte.[8] Nevertheless, despite reporting significant leaps in their photovoltaic efficiencies in recent years, fabrication of organic DSSCs still requires use of toxic solvents and chemicals, is very expensive, and necessitates tight control of processing conditions in a clean-room environment. These challenges greatly limit their range of applications. A potential solution to these challenges involves combining light-harvesting (LH) and reaction center (RC) proteins from photosynthetic organisms with man-made materials in biohybrid devices.[9–12] LH and RC proteins can transduce solar energy toward the generation of a potential difference at quantum efficiencies that approach unity, and a variety of these proteins have been incorporated into devices to harness charge separation for photocurrent generation.[13] For instance, Janfaza et al. combined the LH protein bacteriorhodopsin with TiO_2 nanoparticles in a solar cell and observed an efficiency (η) of 0.35%.[14,15] Likewise, Muthupandian and co-workers reported enhanced photocurrent generation in bacteriorhodopsin-based solar cells incorporating gel electrolytes ($\eta = 0.49\%$) compared to liquid electrolytes ($\eta = 0.19\%$).[16] Alternatively, biohybrid electrodes comprising photosynthetic RC proteins can also be used in the fabrication of DSSCs.[17,18] Similarly, naturally occurring dyes too have been utilized as photosensitizers in DSSCs. For example, when Perez-Donoso and co-workers employed pigments that had been isolated from non-photosynthetic, UV-resistant bacteria, *Hymenobacter* spp. and *Chryseobacterium* spp., as photosensitizers in a DSSC, they observed an overall efficiency of 0.03%.[19] Nevertheless, while the use of LH and RC proteins, aqueous electrolytes,[20] and natural dyes[21] may overcome most of the challenges associated with fabrication of DSSCs, the extraction of proteins from biological hosts, their subsequent purification—often through expensive downstream processing—and preservation of biological function are nontrivial. Moreover, these materials require supporting matrices and covalent linkers in their assembly. As a consequence, not only is the chemical processing that is typically employed to coat proteins and natural dyes onto semiconductors complicated and difficult to scale, but also the devices exhibit poor stability and long-term performance.[22] To this end, we have developed an entirely novel class of biohybrid photovoltaic (bio-PV) materials that can be manufactured economically and sustainably, and can perform at comparable, if not better, efficiencies as biohybrid DSSCs.

2. Results and Discussion

The material that we have developed is biogenic[23,24] and comprises of a porous mesh of *E. coli* BL21 cells that are encapsulated with TiO_2 (**Scheme 1**). The bacterial cells are genetically

Dr. S. K. Srivastava, P. Piwek, S. R. Ayakar, Dr. A. Bonakdarpour, Prof. D. P. Wilkinson, Prof. V. G. Yadav
Department of Chemical and Biological Engineering
The University of British Columbia
2360 East Mall, Vancouver, BC V6T 1Z3, Canada
E-mail: srivastava.research@gmail.com; vikramaditya.yadav@ubc.ca
Dr. A. Bonakdarpour, Prof. D. P. Wilkinson
Clean Energy Research Centre
The University of British Columbia
2360 East Mall, Vancouver, BC V6T 1Z3, Canada
Prof. V. G. Yadav
School of Biomedical Engineering
The University of British Columbia
2360 East Mall, Vancouver, BC V6T 1Z3, Canada
The ORCID identification number(s) for the author(s) of this article can be found under https://doi.org/10.1002/smll.201800729.

DOI: 10.1002/smll.201800729

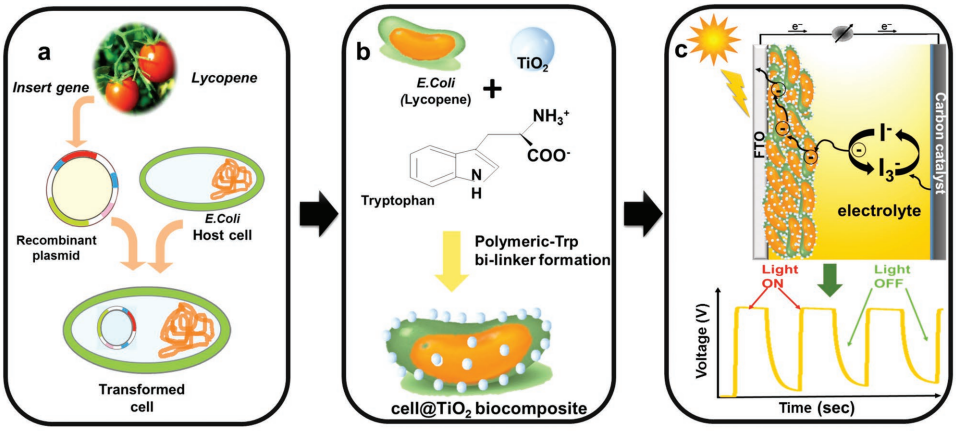

Scheme 1. Sequential representation of the synthesis of whole-cell bio-PV materials highlighting: a) molecular cloning of *E. coli* for expression of lycopene; b) non-covalent surface binding of TiO_2 nanoparticles resulting in core@shell-like morphology; c) deployment of biogenic PV material toward DSSC fabrication.

engineered to synthesize lycopene, a photosensitive dye, and TiO_2 is deposited onto the cells via a tryptophan-mediated supramolecular interface to produce a core@shell-like morphology. The resulting biogenic complex is then coated onto a conductive glass surface (FTO) in the presence of an electrolyte mixture to yield a functioning DSSC. Unlike other biological or biohybrid photovoltaic materials, not only is our synthetic scheme uncomplicated but also the resulting material is exceptionally stable and exhibits impressive PV properties when used as an anode in an I^-/I_3^--based DSSC.

We cloned the lycopene biosynthetic cluster comprising the genes *crtE*, *crtB*, and *crtI* from *Erwinia herbicola* (**Figure 1**b) into an *E. coli* BL21 (DE3) strain that had been previously engineered to express additional copies of the rate-limiting genes of the non-mevalonate (MEP) pathway.[25] Transcription of the lycopene biosynthetic pathway is controlled by a constitutive promoter, whereas transcription of the additional genes of the MEP pathway is driven by a *trc* promoter that is induced with isopropyl β-D-1-thiogalactopyranoside (IPTG).

These modifications generate a strain (referred to, hereinafter, as lyc-*E. coli*) that produces lycopene at yields and titers that are comparable to the best-in-class strains.[26,27] While cells that lack the lycopene pathway do not synthesize the product (Figure 1a), the *trc* promoter is inherently leaky,[28] which implies that the pathways that are transcribed under its control always exhibit a basal activity (Figure 1b). Addition of IPTG fully activates lycopene production, which is confirmed analytically and visually (Figure 1c). Lycopene is a natural carotenoid pigment that provides tomatoes their characteristic orange-red color. It is a highly stable redox pigment that efficiently harvests light and mediates electron transfer. It also absorbs light in the range of 380–520 nm. These properties make it an excellent candidate for use as a photosensitizer in PV and photocatalytic applications.[29,30] Nevertheless, its use in DSSCs has been hitherto limited by the absence of covalent linker groups that can bind it with semiconductors such as TiO_2.[31] We overcame this challenge by coating the bacterial cells with a conductive tryptophan (Trp)-mediated, supramolecular bilayer. This transformation makes the cells more amenable to

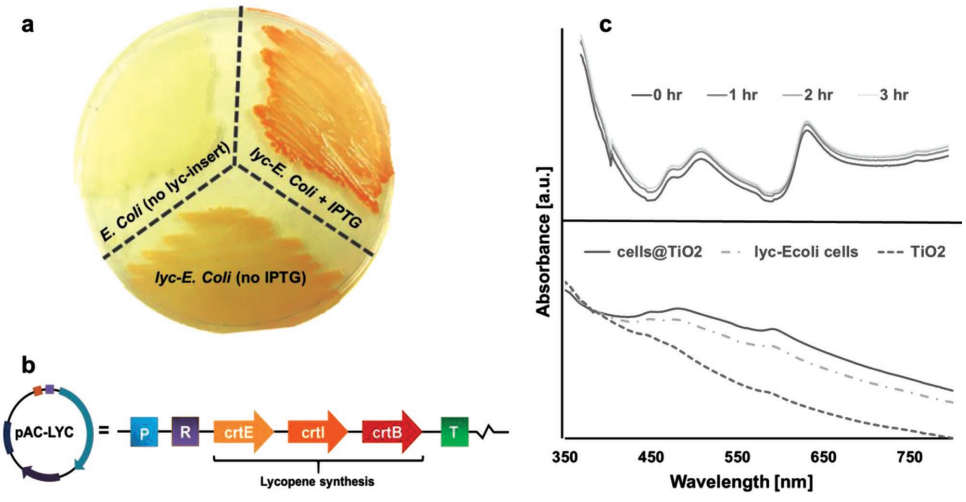

Figure 1. a) Lycopene expression in plates of *E. coli* BL 21 (DE3) cells. b) Genetic construct exhibits a basal level of lycopene production, addition of IPTG stimulates overproduction, which imparts the cells a deep orange-red color. c) We confirmed successful deposition of TiO_2 onto the lyc-*E. coli* cells using UV–vis. The change of absorbance with time (top) and material-specific absorbance spectra (bottom) confirm successful complexation.

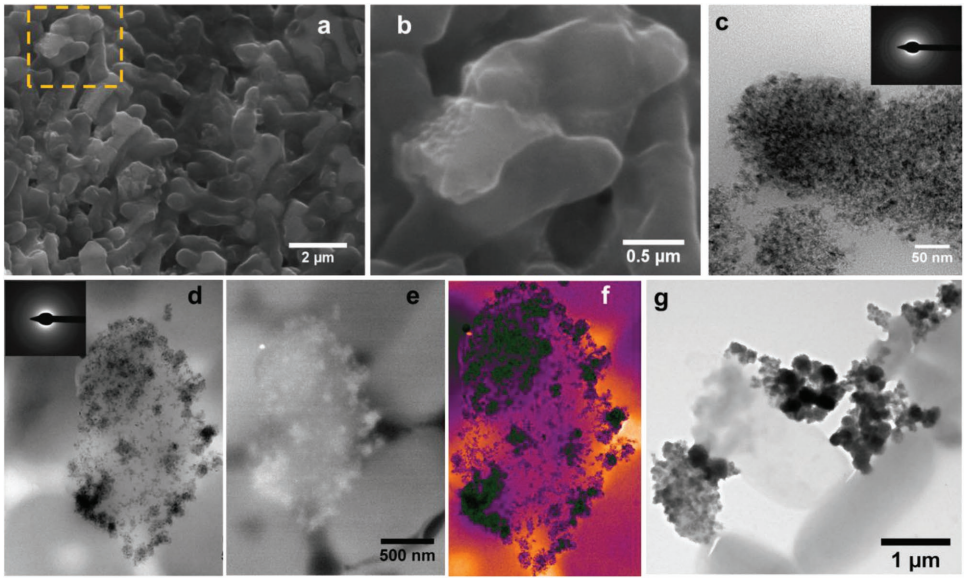

Figure 2. a) SEM image of uniformly coated cells@TiO_2; b) inset of the highlighted region in (a) reveals how individual cells are coated by the TiO_2 NPs; c) TEM image of TiO_2 NPs with a SAED image in the inset; d) bright-field and e) dark-field TEM images of cells@TiO_2 confirm the presence of TiO_2 around the cells; f) a representative false color image of the dark-field TE image clearly shows TiO_2 NPs (black regions) coating the *E. coli* cells (purple mass); and g) bright-field image of multiple TiO_2-coated lyc-*E. coli* cells.

being coated with TiO_2 NPs. Our methodology for anode fabrication is quite distinct from the traditional approach of coating the semiconducting material with the dye or photosensitizer. Trp acts as a highly stable, electrocatalytic bi-linker, and such Trp-mediated interfaces have been previously employed toward the synthesis of core@shell nanoparticles such as Au@(Pd, Pt, Ag, Rh).[32–34]

Accordingly, a colloidal suspension of TiO_2 nanoparticles was synthesized via hydrolysis and condensation of titanium alkoxides in a two-step reaction (Supporting Information). Hydrolysis of the alkoxides and their subsequently polymerization forms a 3D oxide network[35]

$$\mathrm{Ti(OR)_4 + 4H_2O \rightarrow Ti(OH)_4 + 4ROH(hydrolysis)} \quad (1)$$

$$\mathrm{Ti(OH)_4 \rightarrow TiO_2.}x\mathrm{H_2O + (2-}x\mathrm{)H_2O(condensation)} \quad (2)$$

Next, a solution of Trp was mixed directly with cultures of lyc-*E. coli* and colloidal TiO_2 was subsequently added to the mixture. Trp initially forms a polymeric layer around the cells through hydrogen bonding between its indole group and the negatively charged cellular surface. Next, active carboxyl groups within Trp adhere to and reduce the metallic species, which produces a core@shell structure, hereinafter referred to as cells@TiO_2. The formation of cells@TiO_2 was confirmed by UV–vis (Figure 1c, top). The UV–vis spectrum of TiO_2 NPs does not exhibit any absorbance maxima in the visible region, whereas lyc-*E. coli* characteristically absorbs at 450, 485, and 595 nm. Likewise, pure lycopene has an absorption maxima at 450, 475, and 505 nm (Figure S2, Supporting Information). Depositing TiO_2 onto lyc-*E. coli* markedly shifts the latter's UV–vis spectrum, and this transition can be attributed to interfacial rearrangement that occurs during formation of the bilayer of the core@shell morphology. Time-dependent UV–vis scans of TiO_2 NPs, lyc-*E. coli* and cells@TiO_2 further corroborate successful deposition of the NPs onto the cells (Figure 1c, bottom).

Cells@TiO_2 were also analyzed by scanning electron microscopy (SEM), bright-field and dark-field transmission electron microscopy (TEM), and TEM-selected area electron diffraction (SAED) (**Figure 2**). The scanning electron microscopy image of the cells following formation of the Trp-mediated supramolecular interface reveals that TiO_2 neatly and discretely adheres to the individual cells, which are roughly 2 μm in length (Figure 2a,b). SAED also confirms that the TiO_2 particles, which are ≈2–4 nm in diameter and exhibit a characteristic (101) fringe spacing, uniformly coat the cells (Figure 2c). Bright- and dark-field TEM conclusively determine that the TiO_2 layer completely envelops the bacterial cells (Figure 2d–f). We captured dark-field and false color TEM images to confirm the presence of a metal coating around the target cells (Figure 2e,f) on account of a relatively thicker nanoparticle layer. Finally, agglomeration of the cells@TiO_2 into larger structures was confirmed by bright-field imaging (Figure 2g, also refer to Figure S3, Supporting Information, for energy-dispersive X-ray (EDX) analysis).

X-ray diffraction (XRD) was subsequently employed to identify the mineral form of TiO_2 in cells@TiO_2. A comparison between the XRD patterns of cells@TiO_2 and TiO_2 confirms the formation of the TiO_2 NPs (**Figure 3**). The (101) and (110) plane diffraction peaks correspond to anatase and rutile, respectively. The diffraction pattern of TiO_2 matched those in the PDF database (00-021-1272; TiO_2, anatase syn.), with a major peak for (101) at 29.48° followed by minor peaks for (004) at 45.24°, (200) at 56.28°, and (211) at 64.89° (Figure 3c), which confirms synthesis of nanocrystalline anatase (TiO_2), the desired precursor. XRD also confirmed the presence of anatase in the cells@TiO_2 (Figure 3a). Incidentally, cells@TiO_2 also produce a new peak at 22.73° that is not observed in the spectra of either anatase or TiO_2 NPs that are coated with lycopene. Incidentally, lycopene has a major peak at 22.42° corresponding to (311) Bragg's

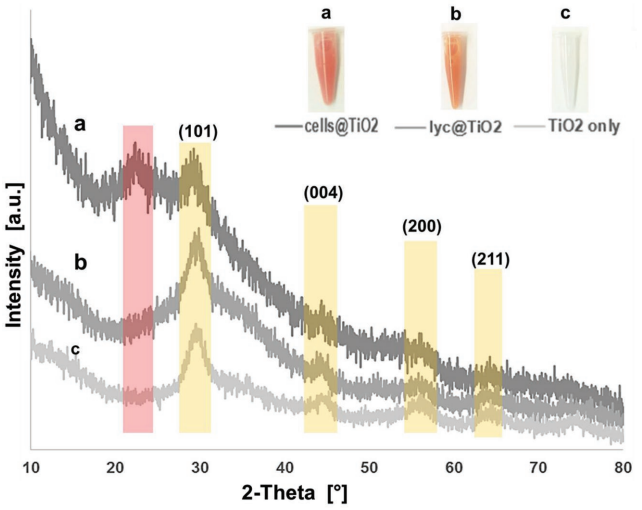

Figure 3. XRD diffraction patterns of a) cells@TiO_2; b) lycopene dye coated over TiO_2; c) TiO_2 NPs.

diffraction. We speculate that the crystals of the intracellular lycopene rearrange following the deposition of TiO_2 onto the cellular surface, which induces a shift in the peak from 22.42° to 22.73° (Figure S5, Supporting Information). This characteristic peak was absent when TiO_2 NPs were coated with extracted lycopene (Figure 3b), which suggests that coating the cells with TiO_2 protects lycopene from thermal degradation.

Finally, the biogenic photovoltaic composite (bio-PV) was coated onto fluorine-doped tin oxide (FTO) glass and pressed between an I^-/I_3^- electrolyte and graphite cathode to investigate its PV properties. We recorded an open-circuit (V_{OC}) potential of 0.289 V, a short-circuit (I_{SC}) current of 0.19 mA, and a corresponding short-circuit current density (J_{SC}) of 0.686 mA cm^{-2} (**Figure 4**a). Further, the difference between light and low light was insignificant, indicating suitability of usage under ambient light conditions.[36] The photocurrent measurements were made under an air mass coefficient of 1.5 (AM 1.5), standard simulated sunlight with precisely controlled active surface area (0.25 cm^2), and continuously calibrated, spectral-mismatch corrected sunlamps, as is the standard in the conventional photovoltaic experimentation.[37] Under these conditions, which closely simulate outdoor sunlight, the total external efficiency (η) for the conversion of incident sunlight to usable electricity was about 0.057%. This efficiency should not be confused with quantum or internal efficiencies, which are usually higher. In fact, despite having a much simpler design and being significantly easier to fabricate, our bio-PV system compares very favorably with another photosensitizer-based bio-PV system developed by Mershin et al., that, according to the authors, was "over four orders of magnitude higher than any PS-based bio-PV till date."[38] The system in Mershin et al. achieved a V_{OC}, η, and J_{SC} of 0.5 V, 0.08%, and 0.362 mA cm^{-2}, respectively, for a similar working area.

The V_{oc} of our bio-PV system can be further enhanced by minimizing dark currents in the DSSC, which are generated owing to a loss of the injected electron from TiO_2, a nanostructured, wide-bandgap semiconductor, to I_3^-, the hole carrier in the solution electrolyte.[39,40] Wu and co-workers have proposed utilization of a bilayer dye using I^-/I_3^- redox as a new design strategy in aqueous p-type DSSCs to address the concerns of both stability and recombination in aqueous phase.[41] Additionally, coating TiO_2 NPs around dye-encapsulating bacteria generates a preponderance of hydrophobic interfaces that significantly increase the resistance of the material (Figure 4a). A similar effect was reported by Palomares and co-workers, who used trifluoroacetic acid (TFA) to create the hydrophobic interfaces in their system.[42] TFA forms a hydrophobic barrier over TiO_2 and impedes direct contact with the electrolyte, which significantly decreases the slope of the corresponding *I–V* curve. We did not detect an *I–V* response when lycopene was coated onto the TiO_2 particles with the same fabrication scheme (Figure S4, Supporting Information), which corroborates our hypothesis that the photocurrent is not attributable

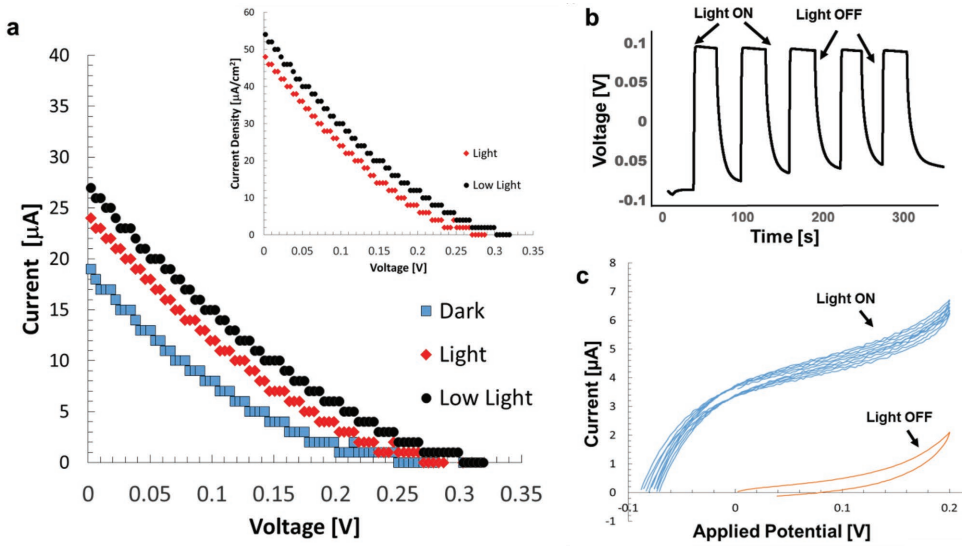

Figure 4. Electrochemical measurements of bio-PV DSSC depicting a) *I–V* curves; b) open-circuit (time dependent) photovoltage response; and c) cyclic voltammetry curves.

to sensitization by the leached lycopene. At any rate, lycopene cannot act as a photovoltaic sensitizer unless it is encapsulated within the cell. The time-dependent (ON/OFF) illumination of the bio-PV DSSC (Figure 4b) exhibited temporal variation of potential when the AM 1.5 illumination was periodically turned on and off every 30 s. This observation confirms the material's PV effect. When illuminated, a net potential difference of about ≈0.2 V was observed over a period of 5 min with minimal decay. We also recorded cyclic voltammograms (CV) to confirm the PV effect (Figure 4c). Moreover, when the illumination was turned off, we observed a capacitive-like voltammogram.[43] However, when the DSSC was illuminated, we measured a current flow of ≈5 μA (≈0.02 mA cm^{-2}). The absence of any reduction-oxidation peaks suggests that the bio-PV material and associated DSSC are fairly stable in the operational range of −0.1 to 0.2 V, which is also the range of the working potential. Our initial study clearly confirms that genetically engineered *E. coli* cells producing lycopene can be coated with TiO_2 NPs for use as the anode of a DSSC with measureable PV effects.

3. Conclusion

The current study demonstrates a novel methodology for rapid and efficient synthesis of a biogenic photovoltaic material that can be incorporated as an anode in a DSSC. While associated PV parameters are of considerable importance, our work directly addresses the challenge of reducing the cost of fabrication of bio-based DSSCs, which have hitherto been high owing to the vagaries in the supply of natural dyes, inconsistencies in the source material, and inefficiencies in extraction.[44,45] Our proof-of-concept study clearly suggests that metallic encapsulation of microbial cells that can synthesize photoexcitable dyes can produce materials with acceptable photovoltaic characteristics. Admittedly, there is considerable room for improvements in the performance of our first-generation material. The external efficiency of the DSSC incorporating cells@TiO_2 is 0.057%, whereas conventional DSSCs typically achieve efficiencies near 13%. Significant gains in efficiency can be expected from the ordered deposition of the biogenic material, use of platinum as the counter electrode, incorporation of coadsorbents into the anode for minimizing dark currents, utilization of MOF complexes as photoactivators, better matching of electrolytes, and use of more light-sensitive dyes.[1] The importance of this study can also be understood as a new perspective by which bio-PV materials can be designed for applications previously limited only to conventional optoelectronics.[46,47] For example, although β-substituted Zn (II) porphyrins achieve solar conversion efficiency of 10.5% when they are incorporated into DSSCs, they suffer from having multistep syntheses that have very low yields compared to thin photovoltaic films.[48–50]

The biogenic synthesis scheme reported herein offers several advantages over other biohybrid photovoltaic systems. Among others, it entirely obviates the need for extraction and purification of dyes, does not require covalent linkages to coating the dye onto conductive particles, and can be easily scaled up in a fermenter. The use of microbial chassis for dye synthesis is also beneficial in regard to improving photovoltaic performance since genome engineering can be employed to increase the yield of the dye or synthesize alternative dyes that can generate greater stoichiometric equivalents of free radicals. Finally, it offers a green chemical route for DSSC fabrication which otherwise utilizes extremely toxic solvents and chemicals, thereby limiting their practical applications. Additionally, elucidation of the material's underlying mechanism of action, its highest occupied molecular orbital-lowest unoccupied molecular orbital (HOMO-LUMO) dependency with redox shuttles and its long-term PV performance are beyond the scope of this preliminary report and will be investigated in future studies. In conclusion, we have combined synthetic biology and biogenic synthesis to fabricate a novel bio-PV material. Our synthesis is rapid, convenient, flexible, and modularizable; and the bio-PV material can be directly incorporated as an anode into DSSCs without any additional downstream processing. This work lays strong foundations for future fundamental and applied research that could eventually spawn a new class of bioorganic optoelectronics.

Supporting Information

Supporting Information is available from the Wiley Online Library or from the author.

Acknowledgements

The authors would like to thank Dr. Protiva R. Roy for her assistance in genetic engineering of *E. coli*; Isaac Martens for his assistance with electrochemical measurements; Dr. Curtis Berlinguette and Valerie Chiykowski for providing access to a solar simulator; and Doug Yuen for his assistance with fabrication of the DSSCs.

Conflict of Interest

The authors declare no conflict of interest.

Keywords

biogenic materials, biohybrid materials, biophotovoltaics, supramolecular assembly, synthetic biology

Received: February 22, 2018
Revised: April 5, 2018
Published online:

[1] G. Calogero, J. H. Yum, A. Sinopoli, G. Di Marco, M. Grätzel, M. K. Nazeeruddin, *Sol. Energy* **2012**, *86*, 1563.
[2] X. Fan, M. Zhang, X. Wang, F. Yang, X. Meng, *J. Mater. Chem. A* **2013**, *1*, 8694.
[3] M. Wright, A. Uddin, *Sol. Energy Mater. Sol. Cells* **2012**, *107*, 87.
[4] H. M. Upadhyaya, S. Senthilarasu, M. H. Hsu, D. K. Kumar, *Sol. Energy Mater. Sol. Cells* **2013**, *119*, 291.
[5] J. Wu, Z. Lan, J. Lin, M. Huang, Y. Huang, L. Fan, G. Luo, *Chem. Rev.* **2015**, *115*, 2136.
[6] G. Calogero, A. Bartolotta, G. Di Marco, A. Di Carlo, F. Bonaccorso, *Chem. Soc. Rev.* **2015**, *44*, 3244.
[7] M. Grätzel, *J. Photochem. Photobiol., C* **2003**, *4*, 145.
[8] M. Ryan, *Platinum Met. Rev.* **2009**, *53*, 216.

[9] D. A. LaVan, J. N. Cha, *Proc. Natl. Acad. Sci. USA* **2006**, *103*, 5251.
[10] F. Wang, X. Liu, I. Willner, *Adv. Mater.* **2013**, *25*, 349.
[11] E. A. Gizzie, J. S. Niezgoda, M. T. Robinson, A. G. Harris, G. K. Jennings, S. J. Rosenthal, D. E. Cliffel, *Energy Environ. Sci.* **2015**, *8*, 3572.
[12] P. I. Gordiichuk, G. J. A. H. Wetzelaer, D. Rimmerman, A. Gruszka, J. W. De Vries, M. Saller, D. A. Gautier, S. Catarci, D. Pesce, S. Richter, P. W. M. Blom, A. Herrmann, *Adv. Mater.* **2014**, *26*, 4863.
[13] B. Mahyad, S. Janfaza, E. S. Hosseini, *Adv. Colloid Interface Sci.* **2015**, *225*, 194.
[14] R. Mohammadpour, S. Janfaza, *ACS Sustainable Chem. Eng.* **2015**, *3*, 809.
[15] K. Deepankumar, A. George, G. K. Priya, M. Ilamaran, N. R. Kamini, T. S. Senthil, S. Easwaramoorthi, N. Ayyadurai, *ACS Sustainable Chem. Eng.* **2017**, *5*, 72.
[16] J. Chellamuthu, P. Nagaraj, S. G. Chidambaram, A. Sambandam, A. Muthupandian, *J. Photochem. Photobiol., B* **2016**, *162*, 208.
[17] Y. Lu, M. Yuan, Y. Liu, B. Tu, C. Xu, B. Liu, D. Zhao, J. Kong, *Langmuir* **2005**, *21*, 4071.
[18] W. Maiaugree, S. Lowpa, M. Towannang, P. Rutphonsan, A. Tangtrakarn, S. Pimanpang, P. Maiaugree, N. Ratchapolthavisin, W. Sang-aroon, W. Jarernboon, V. Amornkitbamrung, *Sci. Rep.* **2015**, *5*, 15230.
[19] N. Órdenes-Aenishanslins, G. Anziani-Ostuni, M. Vargas-Reyes, J. Alarcón, A. Tello, J. M. Pérez-Donoso, *J. Photochem. Photobiol., B* **2016**, *162*, 707.
[20] F. Bella, C. Gerbaldi, C. Barolo, M. Grätzel, *Chem. Soc. Rev.* **2015**, *44*, 3431.
[21] M. R. Narayan, *Renewable Sustainable Energy Rev.* **2012**, *16*, 208.
[22] M. D. Luque de Castro, F. Priego-Capote, *J. Chromatogr., A* **2010**, *1217*, 2383.
[23] S. K. Srivastava, R. Yamada, C. Ogino, A. Kondo, *Nanoscale Res. Lett.* **2013**, *8*, 70.
[24] S. K. Srivastava, M. Constanti, *J. Nanopart. Res.* **2012**, *14*, 831.
[25] J. Yang, L. Guo, *Microb. Cell Fact.* **2014**, *13*, 160.
[26] S. H. Yoon, J. E. Kim, S. H. Lee, H. M. Park, M. S. Choi, J. Y. Kim, S. H. Lee, Y. C. Shin, J. D. Keasling, S. W. Kim, *Appl. Microbiol. Biotechnol.* **2007**, *74*, 131.
[27] P. K. Ajikumar, W. H. Xiao, K. E. Tyo, Y. Wang, F. Simeon, E. Leonard, O. Mucha, T. H. Phon, B. Pfeifer, G. Stephanopoulos, *Science* **2010**, *330*, 70.
[28] G. L. Rosano, E. A. Ceccarelli, *Front. Microbiol.* **2014**, *5*, https://doi.org/10.3389/fmicb.2014.00172.
[29] T. Zhuang, S. Sasaki, T. Ikeuchi, J. Kido, X.-F. Wang, *RSC Adv.* **2015**, *5*, 45755.
[30] G. Richhariya, A. Kumar, P. Tekasakul, B. Gupta, *Renewable Sustainable Energy Rev.* **2017**, *69*, 705.
[31] D. R. Shinde, P. S. Tambade, K. M. Gadave, K. S. Pawar, M. Naushad, H. M. Pathan, *J. Mater. Sci.: Mater. Electron.* **2017**, *28*, 11311.
[32] S. K. Srivastava, M. Guix, O. G. Schmidt, *Nano Lett.* **2016**, *16*, 817.
[33] S. K. Srivastava, T. Hasegawa, R. Yamada, C. Ogino, M. Mizuhata, A. Kondo, *RSC Adv.* **2013**, *3*, 18367.
[34] S. K. Srivastava, J. S. del Rio, C. K. O'Sullivan, C. Ogino, A. Kondo, *RSC Adv.* **2014**, *4*, 48458.
[35] S. Mahshid, M. Askari, M. S. Ghamsari, *J. Mater. Process. Technol.* **2007**, *189*, 296.
[36] M. Freitag, J. Teuscher, Y. Saygili, X. Zhang, F. Giordano, P. Liska, J. Hua, S. M. Zakeeruddin, J. E. Moser, M. Grätzel, A. Hagfeldt, *Nat. Photonics* **2017**, *11*, 372.
[37] S. Ito, P. Chen, P. Comte, M. K. Nazeeruddin, P. Liska, P. Péchy, M. Grätzel, *Prog. Photovolt.: Res. Appl.* **2007**, *15*, 603.
[38] A. Mershin, K. Matsumoto, L. Kaiser, D. Yu, M. Vaughn, M. K. Nazeeruddin, B. D. Bruce, M. Graetzel, S. Zhang, *Sci. Rep.* **2012**, *2*, 234.
[39] A. Stanley, B. Verity, D. Matthews, *Sol. Energy Mater. Sol. Cells* **1998**, *52*, 141.
[40] S. Ito, P. Liska, P. Comte, R. Charvet, P. Péchy, U. Bach, L. Schmidt-Mende, S. M. Zakeeruddin, A. Kay, M. K. Nazeeruddin, M. Grätzel, *Chem. Commun.* **2005**, 4351.
[41] K. A. Click, B. M. Schockman, J. T. Dilenschneider, W. D. McCulloch, B. R. Garrett, Y. Yu, M. He, A. E. Curtze, Y. Wu, *J. Phys. Chem. C* **2017**, *121*, 8787.
[42] A. Sanchez-Diaz, E. Martinez-Ferrero, E. Palomares, *J. Mater. Chem.* **2009**, *19*, 5381.
[43] N. Fattah, H. Ng, Y. Mahipal, A. Numan, S. Ramesh, K. Ramesh, *Materials* **2016**, *9*, 450.
[44] M. Kimura, H. Nomoto, N. Masaki, S. Mori, *Angew. Chem., Int. Ed.* **2012**, *51*, 4371.
[45] H. Hug, M. Bader, P. Mair, T. Glatzel, *Appl. Energy* **2014**, *115*, 216.
[46] D. T. Simon, E. O. Gabrielsson, K. Tybrandt, M. Berggren, *Chem. Rev.* **2016**, *116*, 13009.
[47] S. K. Ravi, V. S. Udayagiri, L. Suresh, S. C. Tan, *Adv. Funct. Mater.* **2017**, 1705305.
[48] G. N. Cohen, *Microbial Biochemistry*, Springer, Berlin **2011**, pp. 487–501.
[49] E. J. Palomares, L. Cabau, V. K. Challuri, A. Moncho, J. N. Clifford, N. Lopez, *Energy Environ. Sci.* **2015**, *8*, 1368.
[50] G. Di Carlo, A. O. Biroli, F. Tessore, S. Caramori, M. Pizzotti, *Coord. Chem. Rev.* **2018**, *358*, 153.

